CellPress

Trends in Molecular Medicine

Review

Cancer Surgery 2.0: Guidance by Real-Time Molecular Technologies

Nina Ogrinc,[1] Philippe Saudemont,[1] Zoltan Takats,[1] Michel Salzet,[1,2,*] and Isabelle Fournier[1,2,*]

***In vivo* cancer margin delineation during surgery remains a major challenge. Despite the availability of several image guidance techniques and intraoperative assessment, clear surgical margins and debulking efficiency remain scarce. For this reason, there is particular interest in developing rapid intraoperative tools with high sensitivity and specificity to help guide cancer surgery *in vivo*. Recently, several emerging technologies including intraoperative mass spectrometry have paved the way for molecular guidance in a clinical setting. We evaluate these techniques and assess their relevance for intraoperative surgical guidance and how they can transform the future of molecular cancer surgery, diagnostics, patient management and care.**

Importance of Clear Margin Delineation and Debulking Efficiency

For solid tumors, surgery remains the first frontline treatment in nearly 80% of diagnosed cases [1]. Many studies have shown that clear surgical tumor margins and debulking via surgery have a drastic impact on patient survival rates. However, surgeons are faced with difficult decision-making with regards to margin delineation and visualization of the actual extension of the tumor. Tumors are normally removed with surrounding healthy tissue margins, wide enough to remove the majority of cancer cells but minimized to prevent the functional loss of the diseased organ. In practice, the margin can vary from 2 mm to 10 cm depending on the type of cancer. Preneoplastic lesions and isolated groups of cancer cells are difficult to detect and are generally missed during surgery [2]. Depending on the site and stage of the primary tumor, forgotten residual cancer cells can lead to immediate re-excision surgery, or to metastasis and bad prognosis [3]. Indeed, after breast-conserving surgery (BCS) it is estimated that around 25% of all patients need re-excision [4], while in colorectal cancer, 17% of the patients experience recurrence after curative surgical resection with clear microscopic margins [5]. In general, it is estimated that the prevalence of positive margins in gastric cancer is up to 20% [6].

It is thus critical to detect with high accuracy the correct localization of the tumor and remaining cells. To that end, surgeons use the information provided by conventional preoperative and intraoperative guidance technologies such as **magnetic resonance imaging** (MRI) (see Glossary), **computed tomography** (CT), or **ultrasound** (US) [7]. Yet, these technologies do not provide the necessary information for complete tumor resection and, therefore, the surgeons still primarily rely on tactile information. However, this is not sufficient to address the problem of discriminating benign and malign, finding the locoregional extension of tumors and managing accurate margin delineation of tumors. Most often this is achieved by intraoperative pathological examination (either gross assessment or histopathological evaluation from frozen sections). Specimen sampling for intraoperative analysis is not trivial and done by the surgeon, which unfortunately already introduces a bias in the process and increases the duration of the surgery.

Therefore, there is an unmet need for intraoperative techniques operating in real time and *in vivo* with sufficient spatial resolution (<1 mm), minimal daily practice interference, and offering operator-friendly

Highlights

Cancer surgery is the first treatment in many solid tumors. Quality of the initial surgery has a strong influence on the patient outcome. Tumors must be excised at best, but accurate delineation of their edges and margin definition is a huge challenge.

Presently, the practice is the intraoperative examination of surgical specimens by the pathologist through morphological examination of stained tissue sections. However, this is far from satisfactory and subjected to an important error rate.

New technologies are emerging for intraoperative assessment, such as traditional tools (US, MRI, and CT) and new modalities (OCT, Raman spectroscopy, and MS).

MS provides the molecular fingerprint of the tissues and molecules appear advantageously as distinct signals. Several MS systems have been developed for intraoperative analysis; for example, iKnife, SpiderMass, and MassSpecPen, which have already been showcased in the operating theater.

[1]University of Lille, Inserm, CHU Lille, U1192 – Protéomique Réponse Inflammatoire Spectrométrie de Masse - PRISM, F-59000 Lille, France
[2]Institut Universitaire de France (IUF), Paris, France

*Correspondence:
michel.salzet@univ-lille.fr (M. Salzet) and
isabelle.fournier@univ-lille.fr (I. Fournier).

instrumentation. To go beyond the anatomy, incorporating real-time molecular information to intraoperative assessment would optimize surgical resection and cancer diagnosis (see Clinician's Corner). In this review we focus on emerging technologies, particularly intraoperative mass spectrometry (MS), which will help guide surgical resection *in vivo* and in real time based on molecular profiles and pave the way of the new gold standards in cancer surgery; Cancer surgery 2.0.

Conventional Cancer Surgery Workflow; Analysis and Pitfalls

Techniques for Image Guidance

Several conventional methodologies are used pre-operatively and intraoperatively for evaluating resection margins and extension of the tumor. A schematic of the tumor resection process and analysis is shown in Figure 1.

To reduce the risk of re-excisions and ensure the successful removal of cancerous tissues, specific technologies for image guidance can be used in the operating room. These are normally 3D preoperative MRI or CT scans projected onto a separate screen [8–11]. These techniques offer the surgeon visualization and detection of tumors in real-time and improve the accuracy of tumor resection without disrupting the normal surgical workflow. However, the acquired images do not always correlate with eye observations due to tumor growth, deformations of soft tissues, shifting of organs, or misalignment of the image display compared to the surgical field. This has partially been resolved by intraoperative MRI and CT systems, especially in neurosurgery [11–13]. However, these systems require a complex infrastructure, specialized surgical suites and instruments due to the magnetic fields. Image guidance techniques are often complemented with routine fluoroscopy and intraoperative US for surgical navigation [14]. US was easily implemented as it provides real-time information and straightforward image interpretation with high sensitivity and specificity [15,16]. US is, nevertheless, an iterative contact-based method, which is less useful for identifying tumor boundaries or microscopic tumors during open surgeries [17].

Intraoperative Histology

Although intraoperative histology assessment is not always routine practice, it remains the most frequently performed examination either by intraoperative frozen section analysis or touch imprint cytology [18]. In an ideal clinical scenario, an accurate diagnosis should be rendered within 5–10 min. However, in most cases it requires 20–40 min depending on sampling procedures and care unit organization. The complete histopathological workup includes embedding in optimal cutting temperature medium, freezing and cutting into sections for best preservation of tissue morphology [18]. Direct freezing of the sample in liquid nitrogen [19] is also possible to reduce the time, but shown to reduce sensitivity by 65–78% during BCS [20]. Hematoxylin and eosin staining of tissues preserves important region-to-region morphology and allows microscopic evaluation of neighboring cell morphology, structure, and organization to derive a diagnosis. Despite using simplified **algorithmic decision trees** interobserver variation persists among experts [21,22]. To improve the accuracy and reduce discordance among specialists **artificial intelligence** (AI) algorithms based on deep neural networks (DNNs) have been recently developed and become a valuable tool for the generation and implementation of complex multi-parametric decision algorithms for pathological analysis [23] (Box 1).

Ambient Ionization Mass Spectrometry: A Newcomer in Cancer Diagnostics

MS is a label-free, robust, and highly sensitive technology used for biomolecular analysis. In MS, the molecules are separated based on their molecular weight. Hence, in one single experiment, thousands of biomolecules can be detected and identified. It has been widely implemented in the medical field for direct microbe identification (biotyping), newborn screening, and quantification of blood circulating drugs and metabolites.

Glossary

Artificial intelligence: intelligence demonstrated by machines (e.g., computers) in contrast to natural intelligence demonstrated by animals and humans.
Algorithmic decision trees: decision support tools that use a tree-like model of decisions and their possible consequences. In pathology, decision trees are used to sufficiently stratify patients into reproducible groups based on tumor phenotypes.
Computed tomography: several X-ray (wavelength 10 nm to 5 pm) scans computed to reconstruct tomography, used in a preoperative context for diagnosis and staging of cancer.
Electrospray ionization: a flow of solvent in which the analyte is present is transferred into a mist of droplets that slowly evaporate to free the molecules in the gas phase. Currents are applied to charge those droplets and transfer them to the analytes.
Fluorescence-guided surgery: visualizes tumors in real time either through autofluorescence, or conventional fluorescent techniques using probes in the visible light spectrum or NIR spectrum. The most common FGSs use targeted probes in the NIR window (700–900 nm) with largest penetration depth of optical light in tissue (5–15 mm).
Magnetic resonance imaging: uses a strong external magnetic field that changes the spin of certain nuclei (mostly hydrogen). During the relaxation it emits radiofrequency that can be measured and imaged.
Matrix-assisted laser desorption/ionization: a laser beam, UV, or IR, is fired against a prepared solution of the analytes together with an absorbing molecule so-called matrix to create a cascade of reactions leading to the transfer of charges to the analytes.
Optical coherence tomography: a high-resolution optical approach using low-coherence light and interferometry to generate cross-sectional depth resolved in 2D and 3D images.
Raman spectroscopy: uses spectral analysis to identify the unique wavelength shift from a monochromatic beam on a tissue backscattered light to identify the molecular signatures (amino acids, lipids proteins and nucleic acids) of tissue that has undergone disease transformation.

The advent of ambient ionization mass spectrometry (AIMS; Box 2) progressively gave more flexibility to the field and broadened its applications. The number of AIMS technologies approved by the US Food and Drug Administration (FDA) has increased over the past years because of their ease of use, with minimal or no sample preparation. Many of these techniques show promise in clinical application for *in vitro* and *ex vivo* analysis including intraoperative analysis; however, they cannot be used for *in vivo* MS-guided surgery. For this purpose, there has been an emergence of real-time AIMS probes, designed for rapid, sensitive, precise, and accurate measurements *in vivo*. Each technique promotes the analyte ions in a distinct way, either by extraction of charged solvent droplets, ultrasonic tissue ablation, laser ablation, laser excitation, laser cutting, or accumulation of smoke. To comply with the clinical settings, all of the probing systems are constituted of a handheld device coupled to a transfer line for ion transfer [24–28] (Figure 2A–E). These probes provide a wealth of chemical information from direct tissue analysis and give tissue specific molecular profiles. The generated molecular barcodes can then be used to assess healthy versus cancer tissue, intratumor heterogeneity, tumor typing and grading, as well as pinpointing metastatic regions. That is, in direct tissue analysis with intraoperative probes, the most favorable is the detection of small molecules such as metabolites and lipids. In general, abnormal lipid metabolism is a common feature of cancer cells and can already be observed at early stages of tumor development [29]. Several fatty acids and lipid species have been shown to be discriminatory in breast [30,31], gastric [32], ovarian cancer [27,28,33,34], brain tumors [35–37], and sarcomas [38]. The probes can be classified depending on the penetration depth, the type of source or by usage either as a surgical cutting or diagnostic screening tool.

Ultrasound: sound waves with frequencies >20 kHz (mainly between 1 and 18 MHz) are used to create images of internal structures of the body by reconstructing the echo coming from tissues bearing various reflection properties.

Stimulated Raman scattering: uses a second light source that induces a stimulated and enhanced scattering of light. It has been used to monitor dynamic changes, alterations in tissue cellularity, axonal density and protein/lipid ratios.

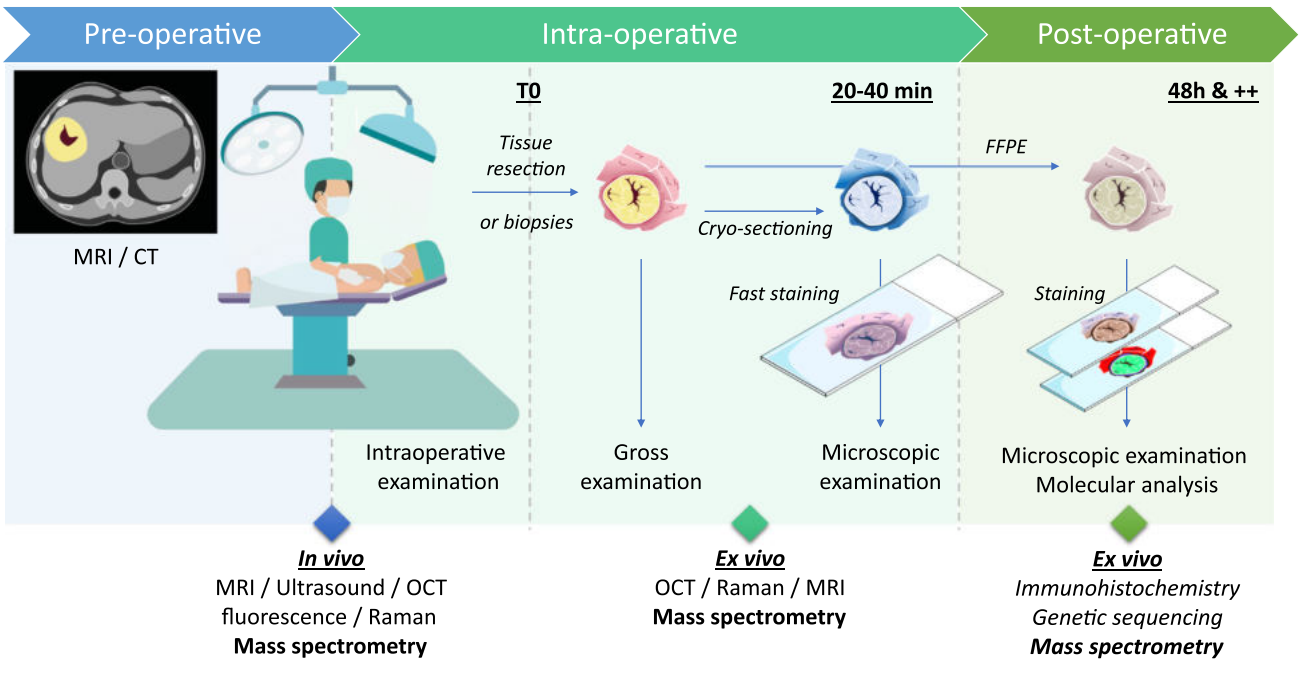

Figure 1. Schematic Representation of Cancer Surgery and the Diagnostic Modalities Involved in Each Step of the Process. Optical imaging techniques are preferred in the preoperative context like MRI and CT scans. In an intraoperative context, the removal of the tumor can be guided by imaging with intraoperative MRI but usually, the tumor piece or biopsies are removed for extemporaneous assessment by the pathologist. Gross examination or sectioning and fast staining/observation are conducted. Then, after the surgery, the classical FFPE histological workflow is unfolded. Emerging modalities in the intraoperative time course are now being used like ultrasound, OCT, Fluorescence, Raman, or mass spectrometry. The tumor drawing and histological slides were adapted from Servier Medical Art (https://smart.servier.com/) and are licensed under a Creative Commons Attribution 3.0 license (CC BY 3.0). Abbreviations: CT, computed tomography; FFPE, formalin-fixed, paraffin-embedded; MRI, magnetic resonance imaging; OCT, optical coherence tomography.

Box 1. Focus on Machine Learning and Deep Learning

Machine learning

In the field of AI, ML represents the development of algorithms that learn from a massive amount of data and experience to improve their predictive values (or accuracy) over time. It is not solely dedicated for classification purposes but in this case, they are conducted in two phases: first is the learning by a training dataset and second, the application of the system on a test dataset and on real cases (Figure I).

Usual ML algorithms rely on a human intervention to be presented with annotated datasets for supervised analysis, with the goal of understanding the rules linking the variables to the annotation in a classification manner. Alternatively, it can rely only on the data without any annotation, in an unsupervised analysis, in which the algorithm needs to determine the underlying structures of the inputs by itself in a clustering manner. The most popular ML approaches for MS cancer-related diagnostics include PCA/LDA models, LASSO for Least Absolute Shrinkage and Selection Operator [90], Partial Least Squares Discriminant Analysis (PLS-DA) [35], Support Vector Machine (SVM) [91], and Random Forest [92]. In general, these methods aim to reduce the complexity/dimensionality of the data itself to make it understandable to human minds.

Deep learning

Among the ML techniques are the deep learning (DL) algorithms that are characterized by the ability to extract useful representation of the data directly from the raw data with reduced preprocessing or human intervention. The most represented methods in DL are the ones derived from neural networks and mostly CNNs, in which the feature discovery and the final task of the model are done in the same training process, making it more powerful. These methods compute several convolutional and nonlinear transformations for the final classification stage of the network [93]. Neural networks are starting to be used in medical imaging because they are well-suited for image-oriented data. In clinical MS, the volume of data available is not yet high enough. Indeed, the power of CNN evolves exponentially with the increasing volume of data, so they work best with large datasets.

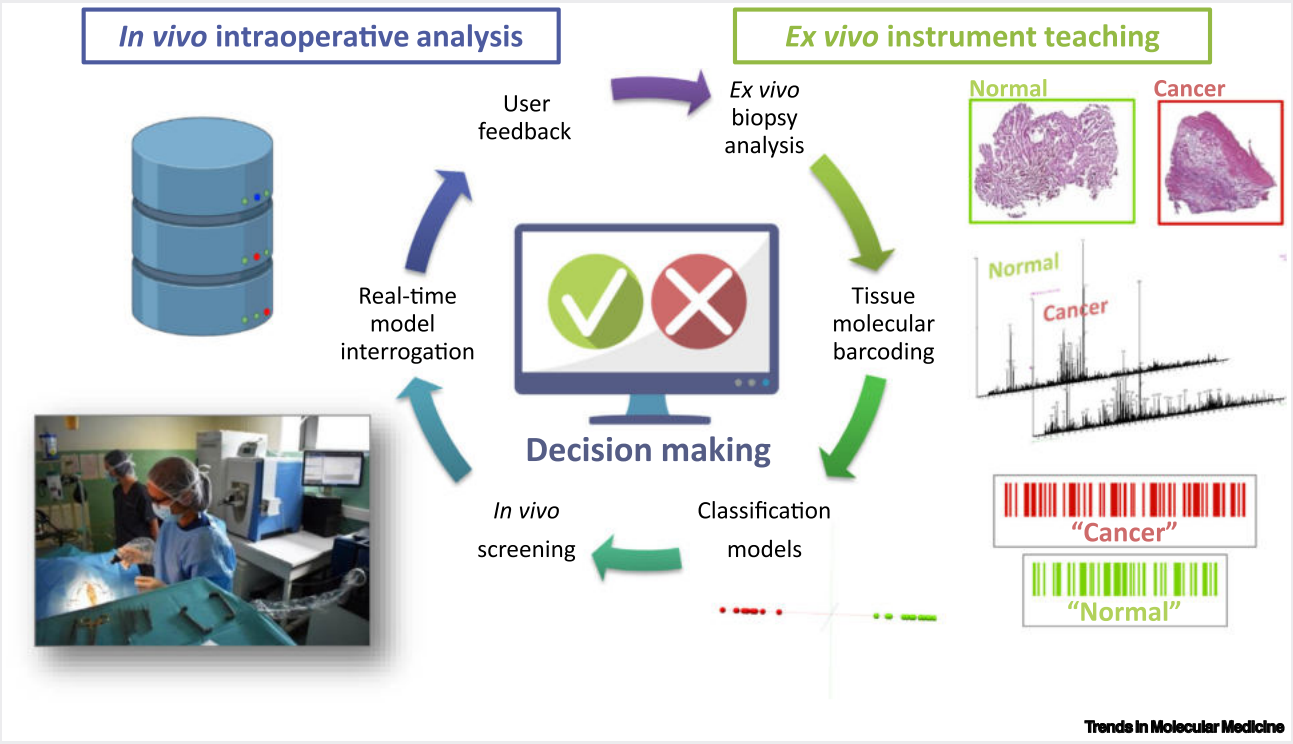

Figure I. Classification Model Construction, Analysis, and Validation Workflow (from Right to Left). The twofold workflow begins with *ex vivo* instrument teaching with analysis of fresh or frozen biopsies or excised tissue (right panel). The samples have preassigned classes given by the pathologists. Each spectrum serves as a molecular barcode. Once an adequate number of samples is analyzed they are subjected to multivariate statistical analysis to build the classification models and perform crossvalidation. Once the model has been built it is used on validation cohorts and on test cohorts then on *in vivo* real subjects (left panel). The model is interrogated in real time and displays user feedback.

Surgical Tool-Based Techniques

The first real-time AIMS probes were introduced based on surgical tools serving as the AIMS source.

Box 2. Guide to AIMS Techniques

A timeline of important MS and AIMS developments is shown in Figure I. They derive from the two main ways of generating ions that are needed for the mass spectrometric analysis; ESI and **matrix-assisted laser desorption ionization** (MALDI). For the benchtop laboratory analysis, desorption and ionization can be achieved by means of:

- a flow of charged solvent droplets applied onto the surface to be analyzed allowing chemicals to be dissolved, ionized, and teared by the gas flow to the MS inlet (DESI) [94] or by a flow of charged gas (direct analysis in real time: DART) [95]
- photons alone: atmospheric pressure MALDI [96]
- combination of photons and ESI: laser-ablation and ESI (LAESI) [97] or MALDI ESI (MALDESI) [98]
- physical probing and ESI: probe electrospray ionization analysis (PESI) [99], needle biopsy, and spray ionization [100]

The techniques show potential and are ideal for benchtop routine analysis of patient samples but cannot be used *in vivo* due to safety, biocompatibility, invasiveness issues, or incompatibility with the size of the sample. Spatial tissue analysis has been possible by the development of several imaging methodologies, for example, DESI-MSI, LAESI, and MALDESI. Out of many, DESI is the most used for chemical imaging and intraoperative diagnosis of tissue samples [101–103]. In the majority of analyzed clinical samples, lipid species encompassing different classes, such as fatty acids and glycerophospholipids, were observed as the discriminating molecules in cancer vs. normal tissue comparison. The demonstration of DESI and DESI-MSI for cancer diagnosis and characterization was conducted on several pathologies including metastatic liver adenocarcinoma, breast, brain, and prostate cancer.

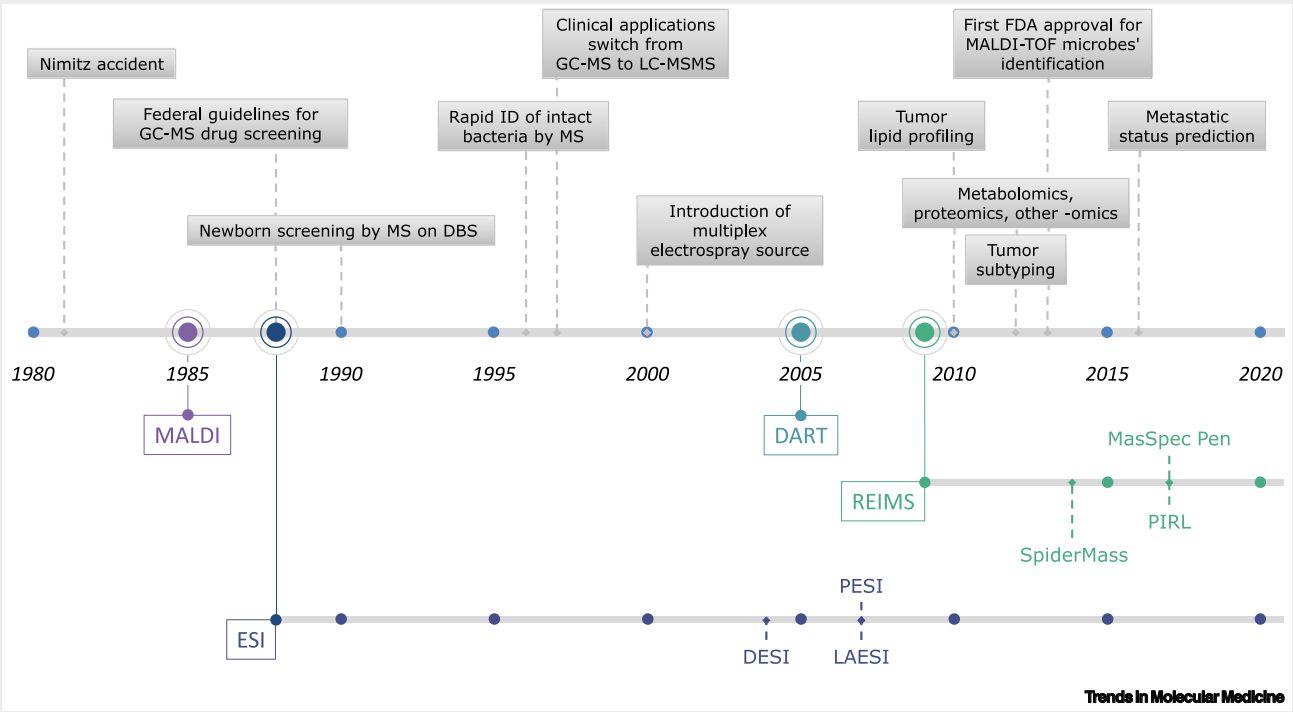

Figure I. General Timeline of Significant Events in the Evolution of MS Toward Clinical Application and FDA Clearance and Approval along with Technical Developments Leading to AIMS and Intraoperative Techniques. It begins with the Nimitz plane accident in which marijuana consumption were detected in the pilots. It led to a zero tolerance against drug uses in the US Army and the increase of drug testing by immunoassays which showed a high rate of false positive. The MS showed promising results and replaced immunoassays in drug testing or newborn disease screening with GC-MS on dried blood spots (DBS) and rapid identification of intact bacteria using MALDI. Meanwhile, the ESI ionization source started to be used and implemented to lower the processing time, the cost per sample and improve the technique turnover. Since 2013, the identification of microbes using MALDI-TOF was approved by the FDA. The second aspect of MS analysis in a clinical environment has been possible by the development of AIMS techniques derived from ESI like DESI, PESI, and LAESI, or from other modalities with the DART, REIMS and the other intraoperative techniques like SpiderMass, PIRL, and the MasSpec Pen that lead to the *in situ* analysis of tumor lipid profiles, tumor subtyping and metastatic status prediction. Partially adapted from https://www.clinicallabmanager.com/trends/clinical-mass-spectrometry/milestones-in-clinical-mass-spectrometry-279.

Stereotactic MS (Figure 2A), developed in 2011, introduced intraoperative desorption **electrospray ionization** (DESI)-MS as a way to validate *in vivo* molecular characterization in a near-real-time intraoperative definition of brain tumor boundaries in surgery [37]. Using a

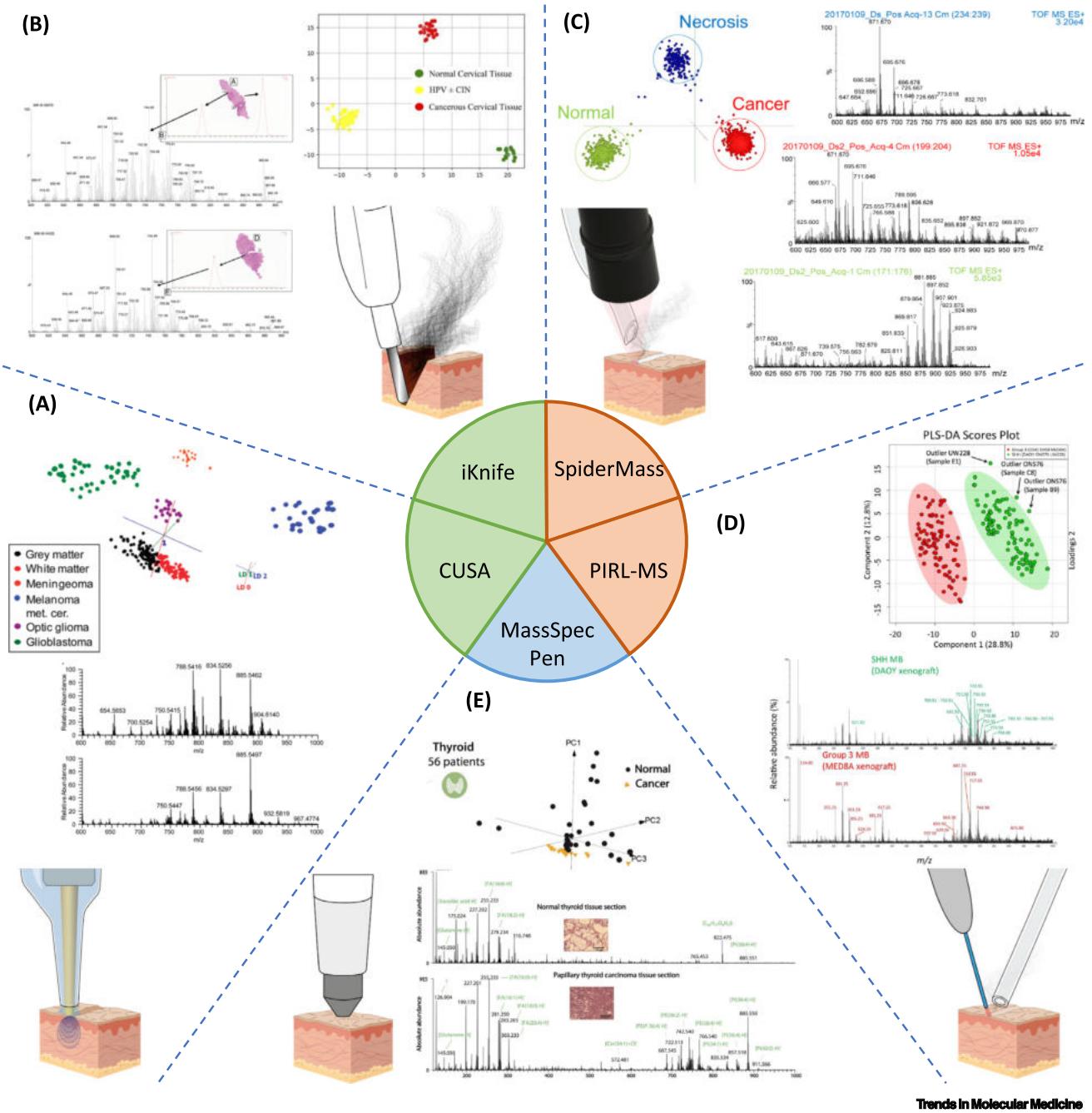

Figure 2. Schematic of AIMS Hand-Held Probes and Their Invasiveness along with Some Examples of Applications. The diverse probes are arranged by their principle of operation: in green are the techniques based on existing surgical tools like CUSA (A) and iKnife (B). In light red represents the IR laser-based techniques such as the SpiderMass (C) and PIRL-MS (D). Blue is the solvent extraction with the MasSpec Pen (E). A close view on the probe and tissue being analyzed is shown with comparable size to visualize the systems invasiveness alongside typical spectra and 3D visualization of the classification models obtained with the technologies. (A) CUSA negative ion mode spectra of human brain gray matter (top) and white matter (bottom) and plot of first three LDA parameters of different human brain tissue samples. Adapted, with permission, from [89] (B) iKnife negative ion mode spectra from benign (top) and malignant (bottom) cervical biopsies and associated LDA model. Adapted, with permission, from [45] (licensed under CC CY-NC-ND 4.0). (C) SpiderMass Positive ion mode mass spectra obtained from necrotic, cancerous, and normal dog sarcoma biopsies and the related LDA score plot representation. Adapted, with permission, from [38]. (D) PIRL-MS spectra collected in the negative ion

(Figure legend continued at the bottom of the next page.)

combination of surgical forceps and cavitron ultrasonic surgical aspirator (CUSA), the specimen is dissected via ultrasonic tissue ablation. Each sampling location is co-registered with preoperative MRI imaging using the GE InstaTrak surgical navigation to correlate specific m/z values to the 3D imaging MRI system. The integrated approach was tested on a human glioma patient [37] and stratification of several glioma surgical cases [39]. The same principle was used to assess glioma subtype, grade, and tumor cell concentration [40], breast cancer margin assessment [41], and meningioma molecular typing [42]. Although the concept is interesting, combining surgical tools with *ex vivo* MS analysis still suffers from the same limitations and issues as intraoperative histology with regards to the specimen sampling and response time.

The Intelligent Knife (iKnife) (Figure 2B) is a concept developed in 2009 for MS-guided surgery combining dissection with analysis [43]. Aerosols are generated by common surgical devices (electrocauterization), and subsequently turned into gas phase ions for MS analysis. They are then transmitted to the MS through plastic tubing. The instrument is equipped with a modified atmospheric interfaces featuring a heated capillary inlet and an orthogonal Venturi-pump aerosol transfer device [25]. The ions are created through the rapid evaporative ionization mass spectrometry (REIMS) interface via a droplet collision on a heated surface [24,44]. The system has been tested *in vivo*, and allowed for confident identification of normal, borderline, and malignant tissues derived from ovary [34], breast [30,31], and cervical cancer [45] patients, as well as endoscopic classification of intestinal wall, cancer, and polyps [32]. The compatibility with common surgical devices is a key advantage of this technique. However, low spatial resolution (0.5–2 mm), destruction of samples during analysis, and in consequence, impossibility for direct crossvalidation with histology are the major drawbacks [46].

Laser-Based Techniques

Lasers are powerful rays of monochromatic and coherent photons. Used in a variety of domains including in medicine, the CO_2 lasers in particular can be used during surgery for precise, fast, bleeding-free cutting or vaporizing of surgical specimens with minimal postoperative pain and edema [47]. Their use has been exemplified in the field of neurosurgery [48], general cancer surgery, skin surgery and eye surgery [47]. The first attempt to use laser probes for real-time MS analysis of *ex vivo* biological tissues was reported in 2011 [49]. The study included divers' lasers (CO_2, Nd:YAG, and nitrogen laser) linked to REIMS interface, as previously described [43]. The systems were tested on food-grade porcine organs, *in vivo* canine carcinoma, and *ex vivo* human colon carcinoma samples [49].

Developed in 2014, the SpiderMass (Figure 2C) is composed of a microsampling probe, transfer line, and an MS analyzer [27]. An infrared laser with a pulse width of 5–7 ns is tuned to 2.94 μm to excite the most intense vibrational band (O-H) of water molecules, in a so-called WALDI (water-assisted laser ionization/desorption) process. The system exhibits low invasiveness: 0.1–0.3 mm^3 is sampled in one experiment and as a result samples are reversibly dehydrated. It is coupled to a laser fiber ending in a handpiece for contact-free screening of any surface *ex vivo* or *in vivo* [26,27,38]. The most typical spectra of direct analysis in both positive and negative ion modes consist of lipid and metabolite species [26]. The SpiderMass system has been applied to analyze *ex vivo* ovarian cancer biopsies and *in vivo* human skin [27]. Moreover, the SpiderMass system was also used to analyze *ex vivo* dog sarcoma samples, allowing for 97% correct

mode from DAOY and UW228 cell lines xenograft and its associated low complexity partial least squares discriminant analysis. Adapted, with permission, from [35]. (E) MasSpec Pen negative ion mode mass spectra obtained from a normal human thyroid tissue section (top) and a papillary thyroid carcinoma tissue section (bottom) alongside a PCA score plots representation for this tissue type. Adapted, with permission, from [28]. Abbreviations: AIMS, ambient ionization mass spectrometry; CUSA, cavitron ultrasonic surgical aspirator; LDA, linear discriminant analysis; PCA, principal component analysis; PIRL-MS, picosecond infrared laser-mass spectrometry.

classification of tumor types and grades [38]. At present, the main disadvantage is the fragility of the bare fiber in the used setup which is prone to breakage.

The picosecond infrared laser (PIRL) was first introduced as a new concept for laser surgery with minimal postoperative scar formation [50]. Later in 2017, a handheld PIRL (Figure 2D) was directly coupled to a MS (PIRL-MS), as for SpiderMass, through a heated inlet [51]. This handheld device relies on a 300-ps impulsion duration that reduces the thermal damage to the tissue providing colder-laser ablation. However, picosecond lasers remain expensive and challenging regarding their fibering due to the peak energy for the injection into the fiber. The system was applied to subcutaneous murine xenograft tumors from different established human meduloblastoma cell lines [35]. A recent study demonstrated that the laser-extracted lipids allow immediate grading of human medulloblastoma tumors into prognostically important subgroups in 10 s. The robustness of the built classification model was tested with the 20% leave out method resulting in 95.53% correct classification rate [36].

Extraction-Based Techniques

The MasSpec Pen (Figure 2E), developed in 2017, follows similar principles as liquid extraction surface analysis and liquid microjunction surface sampling first introduced by Kertesz and Van Berkel [52,53] in 2010. It is an automated, biocompatible, disposable handheld device that allows sampling of tissues by liquid extraction [28]. It is composed of three parts: a syringe pump delivering 4–10 µl of water to the sampling probe, PTFE tubing integrated with valves to transport the water to and from the tissue after a 3-s contact, and a pen-size device for probing the biological tissues. The use of water as solvent allows damage-free extraction of hydrophilic and amphiphilic compounds but requires the probe to be placed in tight contact with the tissue. The MasSpec Pen was used to analyze *ex vivo* human biopsies of breast, thyroid, ovary, and lung cancer and healthy tissue or *in vivo* on mice model samples [28]. The performance of the MasSpec Pen was evaluated for rapid diagnosis of high-grade serous carcinoma where it showed 96.7% clinical sensitivity and 95.7% specificity [33]. Recently, the system was used by seven different surgeons *in vivo* and on excised tissues during 100 surgeries [54].

Statistical Treatment of the Obtained Molecular Data

AIMS probes have been developed to bring MS into the operating room and in the hands of medical personnel. The majority of the described probes are designed for two clinical settings: the first one as an online *in vivo* approach used directly during tumor resection surgeries and the second one as an offline *ex vivo* approach on the bench as a diagnostic tool for clinicians and pathologists [55]. In both *in vivo* and *ex vivo* intraoperative settings, the instrument needs to be trained to recognize cancer cells, types, or grades before used in the clinical setting (Box 1). Then intraoperatively, the device uses its training data to provide an instant feedback to the surgeon. The first (training) step is realized upstream and can be done in the research or clinical laboratory. It requires collection of data from *ex vivo* analysis of tissue sections [26] or whole excised fresh/frozen tissues [25,28] with known diagnostic to enable building a molecular database based on predefined histopathological classes. Once the mass spectra are collected, the molecular profiles can be subjected to different machine-learning (ML) algorithms. For example, principal component analysis in combination with linear discriminant analysis (PCA-LDA) has been used to create molecular databanks and to discriminate normal tissue from cancerous tissues [25,32,46], and to perform sarcoma subtyping and grading [38] and glioma patient stratification [36]. Lasso regression has been used to build classification models on MasSpec Pen data to classify lung cancer, thyroid tumor [28], as well as high-grade serous ovarian cancer versus normal tissue [33]. Recently, ML approaches have been challenged by new end-to-end deep learning algorithms, such as convolutional neural networks (CNNs) where feature extraction and classification can be

learned in one step (Box 1). In the intraoperative context, transfer learning approaches have been explored to improve classification rates of several biological samples including sarcoma subtyping analyzed by the SpiderMass [56].

Once the classification models are built, they can be tested through different crossvalidation techniques and on blind samples. Hence, in a second step, the classification models will be re-interrogated in real time during the surgery. Specific software (i.e., Recognition, MediMass Ltd, LiveID) [26] has been developed to correlate real-time molecular profiles to the prebuilt classification models which will allow for *in vivo* classification during the surgery and prompt a simple readout to the surgeon. The readout is simplified for the clinician; for example, a color-code readout.

Pros and Cons of AIMS Probes Compared to Other Emerging *In Vivo* Guidance Technologies

Concomitantly with AIMS probes, other new technologies based on fluorescence, **optical coherence tomography** (OCT) and **Raman spectroscopy** have emerged for real-time analysis that also hold several interesting features for intraoperative margin evaluation. A comparison of the various hand-held or goggled *in vivo* guidance technologies, in terms of their appropriateness in the intraoperative context, is shown in Table 1.

Fluorescence-guided surgery (FGS) encompasses the broadest range of clinically approved and commercially available imaging systems and fluorophores [57]. Particularly, near-infrared (NIR) and autofluorescence imaging handheld systems such as the photodynamic eye (Hamamatsu Photonics), Fluobeam (Fluoptics), and Artemis (Quest Medical Imaging BV) offer real-time, *in vivo* tumor and surgical margin visualization. The models are operator friendly with low intraoperator variability. Contrary to AIMS probes, fluorescence requires the use of targeted fluorophores to indicate the precise location of primary tumors [58], lymph nodes [59], and aid in surgical resection [60,61]. The use of intrinsic autofluorescence can also indicate specific tissue properties, for example, to identify parathyroid glands [62,63]. An interesting experimental system in its early stages of clinical studies is the fluorescence-goggle assisted imaging and navigation system that allows hands-free operation. The device was first validated in animal studies and later for hepatocellular carcinoma detection in humans [64,65]. It is affordable, portable, user-friendly, and equipped with telemedicine capability (Figure 3A). High-resolution fluorescence imaging has several limitations due to absorption and scattering but offers greater penetration depth than other techniques. The goggled imaging devices show great promise and even permit a hand-free approach opposed to other handheld devices.

OCT is a high-resolution optical approach with similar functionality and use as US. OCT scanners provide iterative quantitative imaging information for intraoperative use [66–68]. A handheld OCT device was used in a multicenter study for *ex vivo* intraoperative assessment of final surgical margin during BCS [69] (Figure 3B). In a translational study, *in vivo* label-free, video-based imaging was introduced by a unique custom-built portable OCT system [70] to assess the BCS margins and the resection bed with >90% mean sensitivity and specificity. The principal difficulties of OCT scanners are sterility and operator stability, which limits the resolution and reproducibility. Indeed, the OCT probe and attached cord need to be wrapped in sterile drapes before being used in the operative field. Sterilization is also mandatory for AIMS probes and except for the laser-based probes, the surgeons are also required to use disposable tips or device to avoid cross-contamination.

Raman and AIMS probes are more closely related with regard to functionality and data acquisition and processing for interpretation. They both provide the ability to detect molecular information for

Table 1. Overview and Comparison of Detection, *In Vivo*/*Ex Vivo* Use, Penetration Depth, Spatial Resolution, Speed, Sensitivity, and Specificity of the Emerging Handheld Techniques

Emerging handheld probes		Detection	*In vivo*/ *ex vivo*	Penetration depth	Spatial resolution	Speed	Sensitivity/ specificity	Refs
Fluorescence-guided surgery	Photodynamic eye (PDE)[a]	ICG fluorescence	*In vivo*	1 cm	~10 μm	Millisecond range	Superficial tissue high sensitivity but decrease with depth	[60,61]
	Fluobeam[a]	ICG or autofluorescence	*In vivo*	1 cm	~10 μm	Millisecond range		[62]
	Artemis[a]	ICG or autofluorescence	*In vivo*	1 cm	~10 μm	Millisecond range		[63]
	Goggle-assisted imaging	ICG fluorescence	*In vivo*	5–15 mm	FOV 12 cm × 10 cm at 5 m working distance	12 frames/s		[64,65]
OCT	Handheld surgical OCT probe	Optical imaging	*In vivo*/ *ex vivo*	1–2 mm	2–10 μm	11.5 frames/s	91.7% sensitivity and 92.1% specificity *ex vivo*	[70]
	Handheld surgical OCT probe	Optical imaging	*Ex vivo*	2–3 mm	<15 μm	>2.3 cm/s scan speed	80% sensitivity and 69% specificity	[69]
Raman	Intraoperative Raman probe	Raman lipid and protein spectra	*In vivo*	1 mm	0.5 mm	0.2 s/three acquisitions	Sensitivity and specificity >90%	[78]
	Optical biopsy needle	Raman lipid and protein spectra	*In situ* during biopsy collection	1 mm	0.5 mm	0.5≠2 s	Sensitivity 80% and specificity 90%	[79]
AIMS handheld probes	i-Knife[a]	Mass lipid and metabolite spectra	*In vivo*/ *ex vivo*	~3.65 mm	0.5–2 mm	3 s	Sensitivity and specificity >90%	[25,26,30–32,44–46]
	SpiderMass	Mass lipid and metabolite spectra	*In vivo*/ *ex vivo*	2–4 μm/ laser shot	400–500 μm	3 s	Sensitivity and specificity >90%	[26,27,38]
	PIRL	Mass lipid and metabolite spectra	*Ex vivo/in situ*	300 μm with 2–10 mm/s movement	~500 μm	10 s	Sensitivity and specificity >90%	[35,36,51]
	MassSpec Pen	Mass lipid and metabolite spectra	*In vivo*/ *ex vivo*	Chemical-extraction-based penetration	0.5–5 mm	3 s	Sensitivity and specificity >90%	[28,33,54]

[a]Commercially available and clinically tested probes. Note that the iKnife is commercially available solely for research purposes.

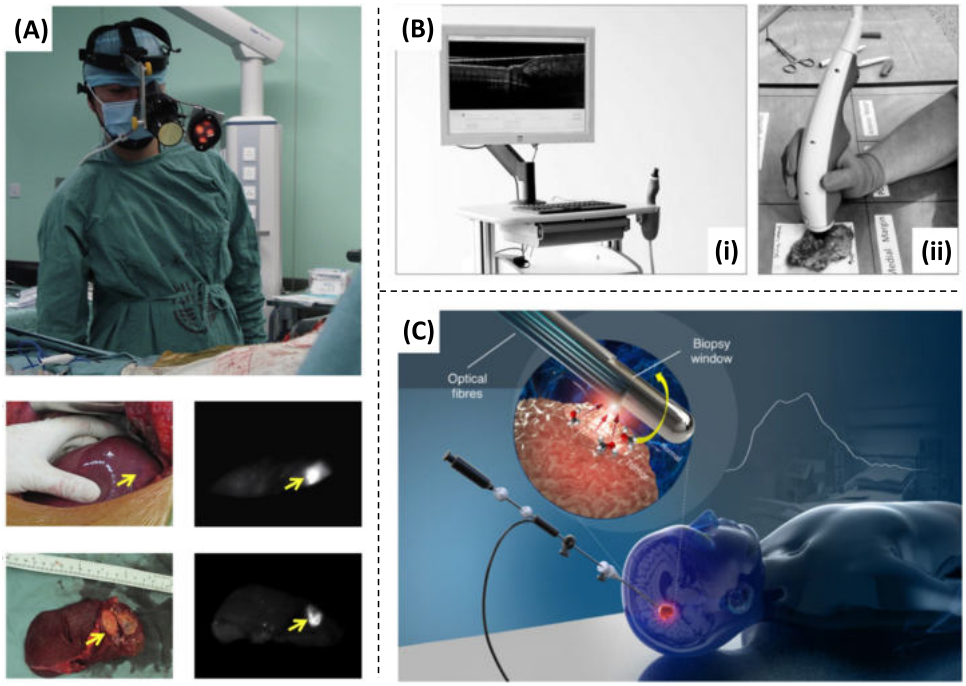

Figure 3. Emerging *In Vivo* Hand-Held Devices for Intraoperative Guidance Based on Optical and Spectroscopic Analysis. (A) Fluorescence-goggle-assisted imaging and navigation system (top). Optical image (bottom left) and fluorescence information (bottom right) displayed in the goggle eyepiece during hepatocellular carcinoma resection. Adapted, with permission, from [65]. Hand-held optical coherence tomography system (i) and *ex vivo* breast shaving margin assessment (ii). Adapted, with permission, from [69]. (C) Hand-held contact Raman spectroscopy probe for *in vivo* assessment during glioma surgery. Adapted, with permission, from [79]. The figure is licensed under a Creative Commons Attribution 4.0 International License.

tissue specific features and hence, distinguish healthy and cancer tissue. Spontaneous and **stimulated Raman scattering** (SRS) have been progressively used in intraoperative cancer diagnosis [71–77]. Although spontaneous Raman is less sensitive than SRS, it has been used for *in vivo* analysis in brain cancer [78,79], real-time analysis of skin and nasopharyngeal carcinoma [80,81], while NIR confocal Raman has been used for investigation of cervical cancer [82]. In particular, the hand-held devices for surgical guidance and *in vivo* fingerprinting are able to distinguish between normal tissue, tumor tissue, and necrosis with accuracies >90% in patients with grade 2–4 gliomas or metastasis associated with lung, colon, and skin cancer [79,83] (Figure 3C). However, Raman requires emission enhancement and proper illumination setup to limit the external light source interference. It also requires sophisticated micrometer-scale light filtering components to extract tissue-specific signatures. Compared to AIMS probes, Raman is not invasive and also offers 2D imaging capabilities or 3D by stacking images or measuring at different depths.

Apart from FGS, most of the Raman and OCT studies were performed *ex vivo* with only one *in vivo* study currently published for both techniques. In contrast, three AIMS systems were evaluated during *in vivo*, real-time analysis in surgery. The iKnife system was first used *in vivo* during canine oncological surgery [24]. The second system, the SpiderMass, was implemented in a veterinary operating theater and tested on a canine patient to evaluate the low invasiveness of the system [38]. The MasSpec pen device was recently used by seven different surgeons and demonstrated *in vivo* during 100

Clinician's Corner

New tools are emerging for intraoperative assessment, which are not traditional medical technologies, such as Raman or MS. These technologies are minimally invasive and could even be operated *in vivo* while avoiding the use of labeled tracers.

MS has demonstrated unprecedented sensitivity and specificity compared to other tools particularly in distinguishing cancer tissues and even providing access to cancer grade, type, or subtype.

New MS devices operating *in vivo* and in real time have recently been developed and were successfully showcased in the operating theater. MS systems provide instant feedback to surgeons and are foreseen as a novel tool for surgery guidance, to accurately delineate the tumor margins and find the locoregional extension of the cancer.

MS systems are based on AI and are trained to recognize cancer cells. Their performances will continue to improve through, in particular, the development of novel deep learning solutions.

Robotics associated with MS devices is the next step for these new tools. They will open the door to new surgical instruments based on a molecular eye for real-time diagnosis. These new devices will help surgeons in their decision-making and will allow personalized patient therapies.

operations [54]. Still, the AIMS probes are facing technical challenges to be addressed such as the portability of such systems and their reproducibility/robustness.

Concluding Remarks

Many efforts have been made in the past decade to improve intraoperative cancer margin delineation and diagnosis. New emerging technologies have shown great potential to pave the way for intraoperative guidance, particularly Raman and MS. For example, intraoperative MS has been shown to provide minute *ex vivo* and *in vivo* analysis of cancer tissue with high specificity and sensitivity. There are, however, still many challenges to be addressed for these technologies to become the next gold standard in cancer surgery. It will include the miniaturization and design of the probes, multicentric studies, the development of imaging, the refinement of bioinformatic solutions and the design of autonomous devices (see Outstanding Questions). We also foresee development of the devices for surgical interventions as add-ons in robotic- assisted tools such as the Da Vinci Robot (Intuitive Surgical) [84] or RoSA (Zimmer Biomet) [85] and combined with AI screening tools for minimally invasive and guided surgery. Some efforts have already been made in that direction with the development of the endoscopic REIMS system [32] and the coupling of the MasSpec Pen with the Da Vinci Robot on a porcine model simulation [86]. Autonomous surgical robots are also a clear direction enabled by SpiderMass-guided surgery [87]. Finally, the future vision for surgery 2.0 is certainly based on autonomous robotic devices for guidance of the MS probe in minimally invasive surgery. Such systems are foreseen to be coupled to augmented reality, as the PIRL-MS in preliminary *ex vivo* experiments with the optical surgical tracking system [88], to provide surgeons with the right decision-making. While there are still many roadblocks ahead before the probes can be widely accepted as medical tools in routine clinical use, the recently developed MS probes are moving toward rapid, ease-of use, and cost-effective solutions for improved patient care.

Outstanding Questions

How can real-time *in vivo* molecular analysis devices be pushed forward to enable intraoperative rapid and real-time *in vivo* imaging? Many of the systems provide point analysis but their development into an imaging modality is mandatory for accurate margin delineation.

How can these different devices be compatible for integration into minimally invasive surgical devices? The systems were generally tested during open surgery. However, there is a clear benefit of minimally invasive surgery for patients, and it is important to find a way to miniaturize the molecular devices to make them compatible with the surgical practices.

How would new AI solutions benefit the real-time molecular systems? AI is indeed foreseen to help with improving the performances of the systems for a better training of the system and more accurate level of information feedback.

Can we take advantage of novel robotic technologies to turn real-time molecular devices into autonomous systems that would be externally piloted by surgeons through augmented reality?

Declaration of Interests

No interests are declared.

References

1. Siegel, R.L. *et al.* (2020) Cancer statistics, 2020. *CA Cancer J. Clin.* 70, 7–30
2. Shin, D. and Park, S.-S. (2013) Clinical importance and surgical decision-making regarding proximal resection margin for gastric cancer. *World J. Gastrointest. Oncol.* 5, 4–11
3. Jacobs, L. (2008) Positive margins: the challenge continues for breast surgeons. *Ann. Surg. Oncol.* 15, 1271–1272
4. Buchholz, T.A. *et al.* (2014) Margins for breast-conserving surgery with whole-breast irradiation in stage I and II invasive breast cancer: American Society of Clinical Oncology Endorsement of the Society of Surgical Oncology/American Society for Radiation Oncology Consensus Guideline. *J. Clin. Oncol.* 32, 1502–1506
5. Pugh, S.A. *et al.* (2016) Site and stage of colorectal cancer influence the likelihood and distribution of disease recurrence and postrecurrence survival: data from the FACS randomized controlled trial. *Ann. Surg.* 263, 1143–1147
6. Raziee, H.R. *et al.* (2012) Systematic review of the predictors of positive margins in gastric cancer surgery and the effect on survival. *Gastric Cancer* 15, 116–124
7. Weissleder, R. and Pittet, M.J. (2008) Imaging in the era of molecular oncology. *Nature* 452, 580–589
8. Grimson, W.E.L. *et al.* (1996) An automatic registration method for frameless stereotaxy, image guided surgery, and enhanced reality visualization. *IEEE Trans. Med. Imaging* 15, 129–140
9. Scheuering, M. *et al.* (2003) Intraoperative augmented reality for minimally invasive liver interventions. In *Medical Imaging 2003: Visualization, Image-Guided Procedures, and Display* (5029) (Galloway, R.L., ed.), pp. 407–417, International Society for Optics and Photonics
10. Nimsky, C. and Carl, B. (2015) Intraoperative imaging. In *Image-Guided Neurosurgery* (Golby, A.J., ed.), pp. 163–190, Academic Press
11. Göksel, O. and Székely, G. (2014) Computational support for intraoperative imaging and IGT. In *Intraoperative Imaging and Image-Guided Therapy* (Jolesz, F., ed.), pp. 63–77, Springer Science & Business Media
12. Nijmeh, A.D. *et al.* (2005) Image-guided navigation in oral and maxillofacial surgery. *Br. J. Oral Maxillofac. Surg.* 43, 294–302
13. Ginat, D.T. *et al.* (2014) 3 Tesla intraoperative MRI for brain tumor surgery. *J. Magn. Reson. Imaging* 39, 1357–1365
14. Mondal, S.B. *et al.* (2014) Real-time fluorescence image-guided oncologic surgery. In *Advances in Cancer Research* (124) (Pomper, M.G. and Fisher, P.B., eds), pp. 171–211, Academic Press
15. van Vledder, M.G. *et al.* (2010) The effect of steatosis on echogenicity of colorectal liver metastases on intraoperative ultrasonography. *Arch. Surg.* 145, 661–667
16. Joo, I. (2015) The role of intraoperative ultrasonography in the diagnosis and management of focal hepatic lesions. *Ultrasonography* 34, 246–257
17. Sahani, D.V. *et al.* (2004) Intraoperative US in patients undergoing surgery for liver neoplasms: comparison with MR imaging. *Radiology* 232, 810–814
18. Pradipta, A.R. *et al.* (2020) Emerging technologies for real-time intraoperative margin assessment in future breast-conserving surgery. *Adv. Sci.* 7, 1901519
19. Nowikiewicz, T. *et al.* (2019) Clinical outcomes of an intraoperative surgical margin assessment using the fresh frozen section method in patients with invasive breast cancer undergoing breast-conserving surgery – a single center analysis. *Sci. Rep.* 9, 13441

20. O'Kelly Priddy, C.M. *et al.* (2016) The importance of surgical margins in breast cancer. *J. Surg. Oncol.* 113, 256–263
21. van den Bent, M.J. (2010) Interobserver variation of the histopathological diagnosis in clinical trials on glioma: a clinician's perspective. *Acta Neuropathol. (Berl.)* 120, 297–304
22. Stoean, C. *et al.* (2019) How much and where to use manual guidance in the computational detection of contours for histopathological images? *Soft. Comput.* 23, 3707–3722
23. Litjens, G. *et al.* (2016) Deep learning as a tool for increased accuracy and efficiency of histopathological diagnosis. *Sci. Rep.* 6, 1–11
24. Balog, J. *et al.* (2010) Identification of biological tissues by rapid evaporative ionization mass spectrometry. *Anal. Chem.* 82, 7343–7350
25. Balog, J. *et al.* (2013) Intraoperative tissue identification using rapid evaporative ionization mass spectrometry. *Sci. Transl. Med.* 5, 194ra93
26. Ogrinc, N. *et al.* (2019) Water-assisted laser desorption/ionization mass spectrometry for minimally invasive in vivo and real-time surface analysis using SpiderMass. *Nat. Protoc.* 14, 3162–3182
27. Fatou, B. *et al.* (2016) *In vivo* real-time mass spectrometry for guided surgery application. *Sci. Rep.* 6, 25919
28. Zhang, J. *et al.* (2017) Nondestructive tissue analysis for *ex vivo* and *in vivo* cancer diagnosis using a handheld mass spectrometry system. *Sci. Transl. Med.* 9, eaan3968
29. Holzlechner, M. *et al.* (2019) Mass spectrometry imaging to detect lipid biomarkers and disease signatures in cancer. *Cancer Rep.* 2, e1229
30. St John, E.R. *et al.* (2017) Rapid evaporative ionisation mass spectrometry of electrosurgical vapours for the identification of breast pathology: towards an intelligent knife for breast cancer surgery. *Breast Cancer Res.* 19, 59
31. Vaysse, P.-M. *et al.* (2020) Stromal vapors for real-time molecular guidance of breast-conserving surgery. *Sci. Rep.* 10, 20109
32. Balog, J. *et al.* (2015) *In vivo* endoscopic tissue identification by rapid evaporative ionization mass spectrometry (REIMS). *Angew. Chem. Int. Ed Engl.* 54, 11059–11062
33. Sans, M. *et al.* (2019) Performance of the MasSpec Pen for rapid diagnosis of ovarian cancer. *Clin. Chem.* 65, 674–683
34. Phelps, D.L. *et al.* (2018) The surgical intelligent knife distinguishes normal, borderline and malignant gynaecological tissues using rapid evaporative ionisation mass spectrometry (REIMS). *Br. J. Cancer* 118, 1349–1358
35. Woolman, M. *et al.* (2017) Rapid determination of medulloblastoma subgroup affiliation with mass spectrometry using a handheld picosecond infrared laser desorption probe †Electronic supplementary information (ESI) available. *Chem. Sci.* 8, 6508–6519
36. Woolman, M. *et al.* (2019) Picosecond infrared laser desorption mass spectrometry identifies medulloblastoma subgroups on intrasurgical timescales. *Cancer Res.* 79, 2426–2434
37. Agar, N.Y.R. *et al.* (2011) Development of stereotactic mass spectrometry for brain tumor surgery. *Neurosurgery* 68, 280–290
38. Saudemont, P. *et al.* (2018) Real-time molecular diagnosis of tumors using water-assisted laser desorption/ionization mass spectrometry technology. *Cancer Cell* 34, 840–851.e4
39. Eberlin, L.S. *et al.* (2013) Ambient mass spectrometry for the intraoperative molecular diagnosis of human brain tumors. *Proc. Natl. Acad. Sci. U. S. A.* 110, 1611–1616
40. Calligaris, D. *et al.* (2013) Mass spectrometry imaging as a tool for surgical decision-making. *J. Mass Spectrom.* 48, 1178–1187
41. Calligaris, D. *et al.* (2014) Application of desorption electrospray ionization mass spectrometry imaging in breast cancer margin analysis. *Proc. Natl. Acad. Sci.* 111, 15184–15189
42. Calligaris, D. *et al.* (2015) Molecular typing of meningiomas by desorption electrospray ionization mass spectrometry imaging for surgical decision-making. *Int. J. Mass Spectrom.* 377, 690–698
43. Schäfer, K.-C. *et al.* (2009) *In vivo*, *in situ* tissue analysis using rapid evaporative ionization mass spectrometry. *Angew. Chem. Int. Ed.* 48, 8240–8242
44. Balog, J. *et al.* (2016) Identification of the species of origin for meat products by rapid evaporative ionization mass spectrometry. *J. Agric. Food Chem.* 64, 4793–4800
45. Tzafetas, M. *et al.* (2020) The intelligent knife (iKnife) and its intraoperative diagnostic advantage for the treatment of cervical disease. *Proc. Natl. Acad. Sci.* 117, 7338–7346
46. St John, E.R. *et al.* (2017) Rapid evaporative ionisation mass spectrometry of electrosurgical vapours for the identification of breast pathology: towards an intelligent knife for breast cancer surgery. *Breast Cancer Res. BCR* 19, 59
47. Fitzpatrick, R.E. and Goldman, M.P. (1995) Advances in carbon dioxide laser surgery. *Clin. Dermatol.* 13, 35–47
48. Belykh, E. *et al.* (2017) Laser application in neurosurgery. *Surg. Neurol. Int.* 8
49. Schäfer, K.-C. *et al.* (2011) *In situ*, real-time identification of biological tissues by ultraviolet and infrared laser desorption ionization mass spectrometry. *Anal. Chem.* 83, 1632–1640
50. Franjic, K. *et al.* (2009) Laser selective cutting of biological tissues by impulsive heat deposition through ultrafast vibrational excitations. *Opt. Express* 17, 22937–22959
51. Woolman, M. *et al.* (2017) Optimized mass spectrometry analysis workflow with polarimetric guidance for *ex vivo* and *in situ* sampling of biological tissues. *Sci. Rep.* 7, 468
52. Berkel, G.J.V. *et al.* (2008) Liquid microjunction surface sampling probe electrospray mass spectrometry for detection of drugs and metabolites in thin tissue sections. *J. Mass Spectrom.* 43, 500–508
53. Kertesz, V. and Van Berkel, G.J. (2010) Liquid microjunction surface sampling coupled with high-pressure liquid chromatography–electrospray ionization-mass spectrometry for analysis of drugs and metabolites in whole-body thin tissue sections. *Anal. Chem.* 82, 5917–5921
54. Zhang, J. *et al.* (2020) Direct molecular analysis of *in vivo* and freshly excised tissues in human surgeries with the MasSpec Pen technology. *medRxiv* Published online December 16, 2020. https://doi.org/10.1101/2020.12.14.20248101
55. Ifa, D.R. and Eberlin, L.S. (2016) Ambient ionization mass spectrometry for cancer diagnosis and surgical margin evaluation. *Clin. Chem.* 62, 111–123
56. Seddiki, K. *et al.* (2020) Cumulative learning enables convolutional neural network representations for small mass spectrometry data classification. *Nat. Commun.* 11, 5595
57. Zhang, R.R. *et al.* (2017) Beyond the margins: real-time detection of cancer using targeted fluorophores. *Nat. Rev. Clin. Oncol.* 14, 347–364
58. Zhang, Y.-M. *et al.* (2017) Liver tumor boundaries identified intraoperatively using real-time indocyanine green fluorescence imaging. *J. Cancer Res. Clin. Oncol.* 143, 51–58
59. Tagaya, N. *et al.* (2011) A novel approach for sentinel lymph node identification using fluorescence imaging and image overlay navigation surgery in patients with breast cancer. *World J. Surg.* 35, 154–158
60. Gotoh, K. *et al.* (2009) A novel image-guided surgery of hepatocellular carcinoma by indocyanine green fluorescence imaging navigation. *J. Surg. Oncol.* 100, 75–79
61. Nanashima, A. *et al.* (2019) Efficacy of hepatic segmental visualization using indocyanine green photodynamic eye imaging. *World J. Surg.* 43, 1308–1312
62. Falco, J. *et al.* (2016) Cutting edge in thyroid surgery: autofluorescence of parathyroid glands. *J. Am. Coll. Surg.* 223, 374–380
63. van Driel, P.B.A.A. *et al.* (2015) Characterization and evaluation of the artemis camera for fluorescence-guided cancer surgery. *Mol. Imaging Biol.* 17, 413–423
64. Liu, Y. *et al.* (2011) Hands-free, wireless goggles for near-infrared fluorescence and real-time image-guided surgery. *Surgery* 149, 689–698
65. Liu, Y. *et al.* (2013) First in-human intraoperative imaging of HCC using the fluorescence goggle system and transarterial delivery of near-infrared fluorescent imaging agent: a pilot study. *Transl. Res.* 162, 324–331
66. Hamdoon, Z. *et al.* (2016) Optical coherence tomography in the assessment of oral squamous cell carcinoma resection margins. *Photodiagn. Photodyn. Ther.* 13, 211–217
67. Bhattacharjee, M. *et al.* (2011) Binary tissue classification studies on resected human breast tissues using optical coherence tomography images. *J. Innov. Opt. Health Sci.* 04, 59–66
68. Kut, C. *et al.* (2015) Detection of human brain cancer infiltration *ex vivo* and *in vivo* using quantitative optical coherence tomography. *Sci. Transl. Med.* 7, 292ra100

69. Zysk, A.M. *et al.* (2015) Intraoperative assessment of final margins with a handheld optical imaging probe during breast-conserving surgery may reduce the reoperation rate: results of a multicenter study. *Ann. Surg. Oncol.* 22, 3356–3362
70. Erickson-Bhatt, S.J. *et al.* (2015) Real-time imaging of the resection bed using a handheld probe to reduce incidence of microscopic positive margins in cancer surgery. *Cancer Res.* 75, 3706–3712
71. Gniadecka, M. *et al.* (2004) Melanoma diagnosis by Raman spectroscopy and neural networks: structure alterations in proteins and lipids in intact cancer tissue. *J. Invest. Dermatol.* 122, 443–449
72. Brozek-Pluska, B. *et al.* (2012) Raman spectroscopy and imaging: applications in human breast cancer diagnosis. *Analyst* 137, 3773–3780
73. Haka, A.S. *et al.* (2006) *In vivo* margin assessment during partial mastectomy breast surgery using Raman spectroscopy. *Cancer Res.* 66, 3317–3322
74. Orringer, D.A. *et al.* (2017) Rapid intraoperative histology of unprocessed surgical specimens via fibre-laser-based stimulated Raman scattering microscopy. *Nat. Biomed. Eng.* 1, 0027
75. Hollon, T.C. *et al.* (2018) Rapid intraoperative diagnosis of pediatric brain tumors using stimulated Raman histology. *Cancer Res.* 78, 278–289
76. Bae, K. *et al.* (2018) Epi-detected hyperspectral stimulated Raman scattering microscopy for label-free molecular subtyping of glioblastomas. *Anal. Chem.* 90, 10249–10255
77. Hollon, T.C. *et al.* (2020) Near real-time intraoperative brain tumor diagnosis using stimulated Raman histology and deep neural networks. *Nat. Med.* 26, 52–58
78. Jermyn, M. *et al.* (2015) Intraoperative brain cancer detection with Raman spectroscopy in humans. *Sci. Transl. Med.* 7, 274ra19
79. Desroches, J. *et al.* (2018) A new method using Raman spectroscopy for *in vivo* targeted brain cancer tissue biopsy. *Sci. Rep.* 8, 1–10
80. Lui, H. *et al.* (2012) Real-time Raman spectroscopy for *in vivo* skin cancer diagnosis. *Cancer Res.* 72, 2491–2500
81. Lin, K. *et al.* (2017) Real-time *in vivo* diagnosis of nasopharyngeal carcinoma using rapid fiber-optic Raman spectroscopy. *Theranostics* 7, 3517–3526
82. Duraipandian, S. *et al.* (2011) *In vivo* diagnosis of cervical precancer using Raman spectroscopy and genetic algorithm techniques. *Analyst* 136, 4328–4336
83. Desroches, J. *et al.* (2015) Characterization of a Raman spectroscopy probe system for intraoperative brain tissue classification. *Biomed. Opt. Express* 6, 2380–2397
84. Lux, M.M. *et al.* (2010) Ergonomic evaluation and guidelines for use of the daVinci Robot System. *J. Endourol.* 24, 371–375
85. Lefranc, M. and Peltier, J. (2016) Evaluation of the ROSA™ Spine robot for minimally invasive surgical procedures. *Expert Rev. Med. Devices* 13, 899–906
86. Keating, M.F. *et al.* (2020) Integrating the MasSpec Pen to the da Vinci Surgical System for *in vivo* tissue analysis during a robotic assisted porcine surgery. *Anal. Chem.* 92, 11535–11542
87. Ogrinc, N. *et al.* (2020) Robot-assisted SpiderMass for *in vivo* real-time topography mass spectrometry imaging. *bioRxiv* Published online December 16, 2020. https://doi.org/10.1101/2020.12.15.422889
88. Woolman, M. *et al.* (2020) *In situ* tissue pathology from spatially encoded mass spectrometry classifiers visualized in real time through augmented reality. *Chem. Sci.* 11, 8723–8735
89. Schäfer, K.-C. *et al.* (2011) Real time analysis of brain tissue by direct combination of ultrasonic surgical aspiration and sonic spray mass spectrometry. *Anal. Chem.* 83, 7729–7735
90. Tibshirani, R. (1996) Regression shrinkage and selection via the lasso. *J. R. Stat. Soc. Ser. B Methodol.* 58, 267–288
91. Cortes, C. and Vapnik, V. (1995) Support-vector networks. *Mach. Learn.* 20, 273–297
92. Breiman, L. (2001) Random Forests. *Mach. Learn.* 45, 5–32
93. Goodfellow, I.J. *et al.* (2014) Generative Adversarial Networks. *ArXiv* Published online June 10, 2014. https://arxiv.org/abs/1406.2661
94. Takáts, Z. *et al.* (2004) Mass spectrometry sampling under ambient conditions with desorption electrospray ionization. *Science* 306, 471–473
95. Cody, R.B. *et al.* (2005) Versatile new ion source for the analysis of materials in open air under ambient conditions. *Anal. Chem.* 77, 2297–2302
96. Laiko, V.V. *et al.* (2000) Atmospheric pressure matrix-assisted laser desorption/ionization mass spectrometry. *Anal. Chem.* 72, 652–657
97. Nemes, P. and Vertes, A. (2010) Laser ablation electrospray ionization for atmospheric pressure molecular imaging mass spectrometry. *Methods Mol. Biol. Clifton NJ* 656, 159–171
98. Sampson, J.S. *et al.* (2006) Generation and detection of multiply-charged peptides and proteins by matrix-assisted laser desorption electrospray ionization (MALDESI) Fourier transform ion cyclotron resonance mass spectrometry. *J. Am. Soc. Mass Spectrom.* 17, 1712–1716
99. Mandal, M.K. *et al.* (2012) Application of probe electrospray ionization mass spectrometry (PESI-MS) to clinical diagnosis: solvent effect on lipid analysis. *J. Am. Soc. Mass Spectrom.* 23, 2043–2047
100. Liu, J. *et al.* (2011) Biological Tissue diagnostics using needle biopsy and spray ionization mass spectrometry. *Anal. Chem.* 83, 9221–9225
101. Santagata, S. *et al.* (2014) Intraoperative mass spectrometry mapping of an onco-metabolite to guide brain tumor surgery. *Proc. Natl. Acad. Sci.* 111, 11121–11126
102. Pirro, V. *et al.* (2017) Intraoperative assessment of tumor margins during glioma resection by desorption electrospray ionization-mass spectrometry. *Proc. Natl. Acad. Sci.* 114, 6700–6705
103. Brown, H.M. *et al.* (2021) Intraoperative mass spectrometry platform for IDH mutation status prediction, glioma diagnosis, and estimation of tumor cell infiltration. *J. Appl. Lab. Med.* Published online February 1, 2021. https://doi.org/10.1093/jalm/jfaa233